Modelling and Performance Assessment of a Thermally-Driven Cascade Adsorption Cycle Suitable for Cooling Applications.

Marcello Aprile ([1,a]), A. Freni[b], T. Toppi[a], M. Motta[a]

[a] Department of Energy, Politecnico di Milano, 20156 Milano, Italy

[b] CNR - Institute of Chemistry of Organo Metallic Compounds (ICCOM), Pisa, Italy

Preprint.

Please cite this paper as:

M. Aprile, A. Freni, T. Toppi, M. Motta, Modelling and performance assessment of a thermally-driven cascade adsorption cycle suitable for cooling applications. Thermal Science and Engineering Progress 19 (2020), 100602. https://doi.org/10.1016/j.tsep.2020.100602

Abstract

Adsorption chillers can provide energy efficient cooling and have large potential for performance increase and cost reduction compared to conventional chillers. Among the different R&D activities currently in progress in the field, the development of advanced cascading adsorption cycles is an effective way to improve the performance of standard adsorption units, making this technology especially interesting in applications where waste heat for driving the adsorption chiller is a widely available, such as many industrial processes, cogeneration plants, I.C. engines, district heating networks. In this paper, a novel modelling tool able to simulate complex adsorption cycles is presented and validated with literature data. The simulation tool is used to investigate numerically the performance of a cascade adsorption cycle consisting of a twin

[1] Corresponding author

E-mail address: marcello.aprile@polimi.it

adsorber high-temperature cycle with heat recovery coupled with an intermittent adsorber low-temperature cycle. A parametric analysis is carried out showing the optimization potential in terms of Coefficient Of Performance (COP) and specific cooling power (SCP) with varying cycle periods, step time ratios and adsorbent mass ratios. COP of 0.97 with SCP of 142 W/kg are found for water-zeolite 4A (high-temperature) and water-CaCl2/Silica gel (low-temperature cycle). These results are in line with previous findings reported in literature. Finally, useful recommendations for further performance improvement are provided.

1. Introduction

Adsorption cooling technology is very attractive for industrial/automotive waste heat recovery, solar thermal or geothermal energy utilization, mainly due to the ability to be driven by relatively low temperature heat source [1]. Adsorption is a spontaneous physical phenomenon in which a vapor (adsorbate) is reversibly adsorbed onto a porous solid media (adsorbent). The advantages deriving from the use of this technology for heating and cooling are numerous, including the use of benign refrigerants (e.g. water), not hazardous materials (e.g. silica gel, zeolites), no formation of by-products and simple management of the entire process. With respect to liquid absorption, adsorption cycles have no moving parts without the operating limit imposed by solution crystallization.

Adsorption systems suffer, however, from technological limitations that cause a reduction in efficiency in the thermal energy recovery, which is mainly dependent on two factors [2]:

1) the poor heat and mass transfer efficiency of the standard adsorbent bed made of loose adsorbent grains, affecting the adsorption unit specific cooling power (SCP);

2) the intermittent nature of the basic reversible adsorbent cycle (the so called single-effect cycle), affecting the coefficient of performance (COP).

Poor heat and mass transfer effectiveness involves the use of a large quantity of solid adsorbent with the consequent need to produce bulky and heavy adsorption units. Nowadays, many studies proved that intensification of heat transfer properties of the adsorbent bed can be efficiently achieved though preparation of thin adsorbent coatings [3, 4], highly conductive foams [5] or fibers [6, 7], which permitted to design adsorbent units with enhanced power density [8, 9]. A recent research line aims at improving the mass transfer rate through the adsorbent coating by directed mass transfer channels [10].

On the other hand, many efforts have been devoted to develop advanced adsorption cycles (internal heat recovery, mass recovery, thermal wave, cascading cycles) in order to overcome the discontinuity of the basic intermittent cycle and significantly reduce the amount of heat needed for the regeneration phase, thus improving the COP of the adsorption chiller [11]. Employment of two adsorbent beds working in counterphase is commonly adopted to guarantee continuous useful effect, thus overcoming the intrinsic intermittent nature of the basic ad/desorption process. Generally, the twin adsorbent beds are connected to a single evaporator and condenser, generating the well-known double-effect adsorption machine, which is the most common configuration presented in literature [12-15]. Typical cooling COP values of 0.45-0.55 at desorption temperature of 70 –95 °C and SCP 100-180 W/kg were experimentally evaluated under different working conditions and considering a standard pelletised silica gel/water adsorbent [16]. Noticeably higher SCP values in the range 200-1000 W/kg can be achieved by adopting more thermally efficient adsorbent bed configurations [17].

In order to enhance the COP of a double effect adsorption chiller, internal heat recovery cycles are realized by simply transferring the heat from one bed to the other during the isosteric heating/cooling phases, until a fixed difference of temperature □T between beds is reached [18].

Differently, the internal mass recovery cycle is based on the pressure swing between the two adsorbent beds to improve the adsorption chiller COP [19, 20]. Wang et al. demonstrated that the COP of internal heat and mass recovery cycles can reach a maximum increase of 25% and 10%, respectively [21].

Thermal wave cycles are based on the division of adsorption chambers into several modular units [22], so that the fluid follows a multi-step path, which maximizes the difference between inlet and outlet temperatures. In this way, the thermal flux is used efficiently and the recovery of up to 70% of desorption heat is possible [23]. However, a complicated layout of the system has limited the practical use of thermal wave cycles [24].

Multi-stage, multi-bed adsorption systems based on the silica gel/water working pair were proposed in [25, 26] demonstrating the effective use of waste heat at low temperature between 40 and 95 °C as the driving heat sources.

Cascading cycles consisting of the superposition of a twin adsorber high temperature (HT) cycle and an intermittent or twin adsorber low temperature (LT) cycle were proposed and demonstrated in [27]. Liu and

Leong [28] investigated a cascading cycle consisting of a twin adsorber, zeolite-water, HT cycle with heat and mass recovery and an intermittent adsorber, silica gel-water, LT cycle. Uyun et al. [29] investigated the performance of an advanced cascading adsorption cycle consisting of a twin adsorber HT cycle and a twin adsorber LT cycle with mass recovery.

In this work, the objective is to develop a transient modular modelling approach to simulate complex adsorption cycles for adsorption cooling applications based on STACY, an object-oriented code originally developed for steady-state simulation of liquid absorption cycles [30]. The developed tool presents some original features such as: i) a new module to simulate the coupled heat and mass transfer processes through the adsorbent bed, ii) a new library including the adsorption data of a range of adsorbent/adsorbate working pairs, iii) new settings for transient simulation (number of cycles, cycle time, ad/desorption step time ratio), iv) simulation of the operational mode of pumps and switching valves installed in the external hydraulic circuit.

Firstly, the tool was validated with literature data, and then used to simulate a cascade adsorption cycle consisting of a twin adsorber high- temperature (HT) cycle with heat recovery coupled with an intermittent adsorber low-temperature (LT) cycle. A numerical procedure was established for the optimization of COP and specific cooling power (SCP) of the cascading cycle with varying cycle periods, step time ratios and adsorbent mass ratios. The influence of these parameters was analysed in detail for the pairs Zeolite 4A-water (HT cycle) and CaCl2/Silica gel- water (LT cycle).

2. Mathematical model

The functionalities of a simulation tool originally developed for liquid absorption systems (STACY, [30]) are extended to perform dynamic simulations of adsorption cycles. Derivatives are added to selected state points (i.e., capacitive nodes) and a transient solver is implemented based on the Runge-Kutta numerical method. The solver integrates the differential equations iterating over an integral number of adsorption cycles until the integral mass balances in capacitive nodes vanish. Two new key modules are created, the sorption bed and the capacitive heat exchanger. The first module represents a volume of adsorbent material with uniform properties that can be combined in a modular way with other modules to simulate systems of various

complexity. The second one is used to reproduce the pressure variations inside evaporators and condensers during transients. Lastly, the library of fluids is updated with the sorbent/sorbate pairs described in [31, 33]..

2.1 Sorption bed

The sorption bed module contains two separated fluid domains, one for the heat transfer fluid (HTF) and one for the sorbent/sorbate pair (SW), and four ports as shown in Fig. 1. The HTF domain communicates with ports 1 (inlet) and 2 (outlet) and is internally discretized in a number N of equally sized capacitive nodes. The SW domain consists in one lumped capacity node (5) and communicates through ports 3 (inlet) and 4 (outlet) that represent, respectively, the high-pressure and the low-pressure valves through which refrigerant leaves, during desorption, and enters, during adsorption, the sorption bed.

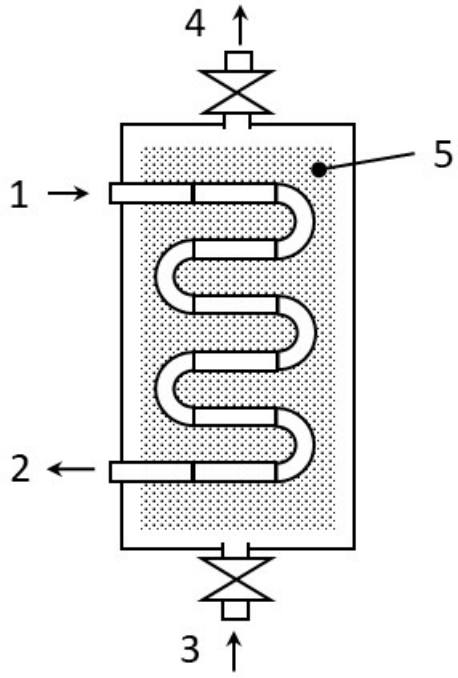

Figure 1 – Sorption bed module: 1) HTF inlet,) HFT outlet, 3) vapor inlet, 4) vapor outlet, 5) sorbent/sorbate node.

It shall be noted that the direction of the refrigerant mass flow through ports 3 and 4 is purely conventional, since in a real unit there are situations in which the refrigerant enters from port 4 or leaves from port 3. Therefore, port 3 and 4 are bidirectional, meaning that these ports carry mass flow rate and pressure as

common variables, and a pair of variables for each transported property (e.g. enthalpy). In each pair of variables, one is the property transported in the direction of the positive mass flow rate, the other is the one transported in the direction of the negative mass flow rate. For example, enthalpy is normally transported from the evaporator in the bed through port 3 but can also leave the bed from the same port if the low-pressure valve is opened when bed pressure is higher than evaporator pressure. To simplify the mathematical formulation of the model, angle brackets are used to indicate the net transfer across the port,

$$\langle \dot{m}h \rangle_3 = \dot{m}_3^+ h_3^+ + \dot{m}_3^- h_3^- \quad (1)$$

where $\dot{m}_3^+ \geq 0$, $\dot{m}_3^- \leq 0$, h_3^+ is the enthalpy at the evaporator outlet and h_3^- is the enthalpy of the vapor in the bed. Through this formalism, the modular approach to system modelling is preserved.

Neglecting the influence of vapor phase and assuming uniform temperature in the bed (including heat exchanger, sorbent and sorbate), the states of the generic SW node are governed by sorbate mass balance and bed enthalpy balance:

$$M_s \frac{dw}{dt} = \langle \dot{m} \rangle_i - \langle \dot{m} \rangle_o \quad (2)$$

$$M_s \frac{dh_{sw}}{dt} + (Mc)_{hx} \frac{dT_{sw}}{dt} = Q_{in} + \langle \dot{m}h \rangle_i - \langle \dot{m}h \rangle_o \quad (3)$$

Additionally, the sorption bed module is equipped with valves (see ports 3 and 4 in Fig. 1). The opening of the valves can be externally imposed through a control signal or, ideally, be determined by the pressure difference between the bed and the external pressures, i.e. the high- pressure valve opens when the pressure difference is positive by a small amount and the low-pressure valve opens when a small negative pressure is set across the valve. After a valve opens, mass transfer between the bed and the connected compartment (i.e., condenser or evaporator) is governed by the linear driving force kinetic equation:

$$\frac{dw}{dt} = M_s(w_{eq} - w)/\tau \quad (4)$$

Where τ is a temperature dependent time constant whose expression is reported e.g. in [31] and w_{eq} is sorption capacity in equilibrium with the temperature of bed and the pressure of the vapor, which is assumed equal to that of the connected compartment. The relationships for w_{eq} are provided in sub-section 2.4. The enthalpy of the sorbent sorbate mixture is:

$$h_{sw} = h_s + w\, h_w \quad (5)$$

Assuming heat of adsorption independent from sorption capacity and ideal gas behaviour for h_v:

$$h_{sw} = c_s T + w(h_v - \Delta H_{ads}) \tag{6}$$

Combining Equations 2–6, the expression for the derivative of bed temperature with time can be derived. The heat input Q_{in} is the sum of elementary contributions $Q_{in,j}$ calculated for each HTF volume.

$$Q_{in,j} = \frac{UA}{N}(T_j - T_{sw}) \quad j = 1..N \tag{7}$$

Lastly, the temperature derivative of each element j is updated according to the following equation:

$$\frac{M_{htf}}{N}\frac{dh_{htf,j}}{dt} = (\dot{m}h)_{htf,j-1} - (\dot{m}h)_{htf,j} - Q_{in,j} \quad j = 1..N \tag{8}$$

2.2 Capacitive heat exchanger

A simple capacitive heat exchanger module is introduced to simulate the dynamic behaviour of evaporator and condenser. The module is constituted of an HTF domain, discretized in N equally sized volumes, and a single node refrigerant domain. The two-phase refrigerant is treated like quasi-compressible, in the sense that the mass inventory can vary but vapor phase is neglected in energy conservation. Since condenser inlet and evaporator outlet are bidirectional ports, angle brackets are used to indicate net transfer of the generic property at a given port section. Mass balance and enthalpy balance can be set as follows:

$$\frac{dM_r}{dt} = \langle \dot{m} \rangle_{r,i} - \langle \dot{m} \rangle_{r,o} \tag{9}$$

$$M_r \frac{dh_r}{dt} + h_r \frac{dM_r}{dt} + (Mc)_{hx}\frac{dT_r}{dt} = \langle \dot{m}h \rangle_{r,i} - \langle \dot{m}h \rangle_{r,o} + Q_{in} \tag{10}$$

In the above expression, $(Mc)_{hx}$ is the thermal capacity of the heat exchanger material, which is supposed to be at refrigerant temperature, and h_r is the enthalpy of saturated liquid refrigerant. The refrigerant enthalpy values at the outlet are set equal to saturated liquid (condenser) or vapor (evaporator). The mass flow rate at inlet and outlet are set externally. For the condenser, it is assumed that outlet mass flow rate equals inlet mass flow rate when the mass inventory is higher than the initial inventory. Heat input and HTF domain are treated as shown in Eq. 7 – 8. The above equations can be combined with the saturation temperature pressure relationship to provide the time derivative of temperature or pressure.

2.3 Working pairs

Equilibrium relationships are given according to a Clausius–Clapeyron phenomenological law [34],

$$ln(P/P_0) = A(w) + \frac{B(w)}{T} \quad (11)$$

where

$$A(w) = a_0 + a_1 w + a_2 w^2 + a_3 w^3 \quad (12)$$

$$B(w) = b_0 + b_1 w + b_2 w^2 + b_3 w^3 \quad (13)$$

The coefficients for the working pairs used in this work, Zeolite 4A- water and $CaCl_2$/Silica gel-water, are shown in Table 1, along with specific heat of dry adsorbent and isosteric heat of adsorption.

Table 1 – Working pairs parameters.

Parameter	Zeolite 4A-water	$CaCl_2$/Silica gel-water
a_0	14.9	
a_1	95.41	13.87
a_2	-636.7	46.46
a_3	1848.8	-105.7
b_0	-7698.8	83
b_1	21498	-3975.9
b_2	-184600	-12550
b_3	512600	31490
c_s	950 J/kg·K	1000 J/kg·K
ΔH_{ads}	3300 kJ/kg	2900 kJ/kg

Additionally, for comparison with previous works, the following empirical isotherm for the pair silica gel-water is implemented [35]:

$$w = A(T)\left[\frac{P_v}{P_{sat}(T)}\right]^{B(T)} \quad (14)$$

where:

$$A(T) = a_0 + a_1 T + a_2 T^2 + a_3 T^3 \quad (15)$$

$$B(T) = b_0 + b_1 T + b_2 T^2 + b_3 T^3 \quad (16)$$

The coefficients of the equilibrium correlations and the heat of adsorption are reported in [30].

2.4 Validation

The model is first used to predict the behaviour of the classical twin bed sorption unit. After initialization of pressures and sorption capacity, the model converges easily to a steady-state cyclical solution, with overall energy and mass balance errors lower than 0.1%. To further validate the correct implementation of the equations and the accuracy of the numerical solution, a model that follows a similar mathematical approach is selected from the literature [30, 31] and model-to-model comparison is performed. The input parameters used in the present model are shown in Table 2. The control strategy of the system is defined as follows. The cycle time is set at 450 s. At cycle start, both valves of each bed are closed. After a switching period of 30 s, the high-pressure valve of the heated bed and the low-pressure valve of the cooled bed are opened. At the end of the cycle, the beds swap their roles by switching the valves specifically installed in the external hydraulic circuit.

Table 2 – Input parameters for model validation [31].

Parameter	Value	Unit
M_s	47	kg
$\dot{m}_{cw,chw}$	2560	kg/h
$\dot{m}_{cnd}$	4930	kg/h
$\dot{m}_{hw}$	4610	kg/h
$\dot{m}_{cw,bed}$	5470	kg/h
UA_{evp}	5345	W/K
UA_{cnd}	16872	W/K
UA_{bed}	4300	W/K
$T_{chw,i}$	14.8	°C

$T_{hw,i}$	86.3	°C
$T_{cw,i}$	31.1	°C
Mc_{evp}	5250	J/K
Mc_{cnd}	10036	J/K
Mc_{bed}	20460	J/K
$M_{w,evp}$	8.4	kg
$M_{w,cnd}$	16.2	kg
$M_{w,bed}$	16.3	kg
$M_{r,cnd}$	12.2	kg
$M_{r,evp}$	50.0	kg

The Dühring diagrams are compared and very good agreement is found (see Fig. 2). From the diagrams it can be noticed that, after the heating phase, the high-pressure valve is opened slightly before the two pressures in bed and condenser are equalized. Consequently, the bed experiences a sudden increase of the pressure and a small amount of refrigerant flows in from the condenser and gets adsorbed. Afterwards, during the desorption phase, the pressure is set by the condenser. The initial pressure increase is due to the high refrigerant flow rate and the limited heat transfer coefficient between coolant and refrigerant. At the end of desorption, both valves are closed, and the bed is cooled. Similarly, during the cooling phase the low-pressure valve is opened in advance, causing this time a sudden drop in pressure and the release of refrigerant that condenses in the evaporator. During the adsorption phase, pressure is set by the evaporator, and the large refrigerant flow rate at the beginning of the process is responsible for the initial decrease of evaporator pressure. As soon as the low-pressure valve is closed, the bed quickly reaches its equilibrium pressure and the small pressure drop at the end of the process witnesses that mass transfer was taking place just before valve closing.

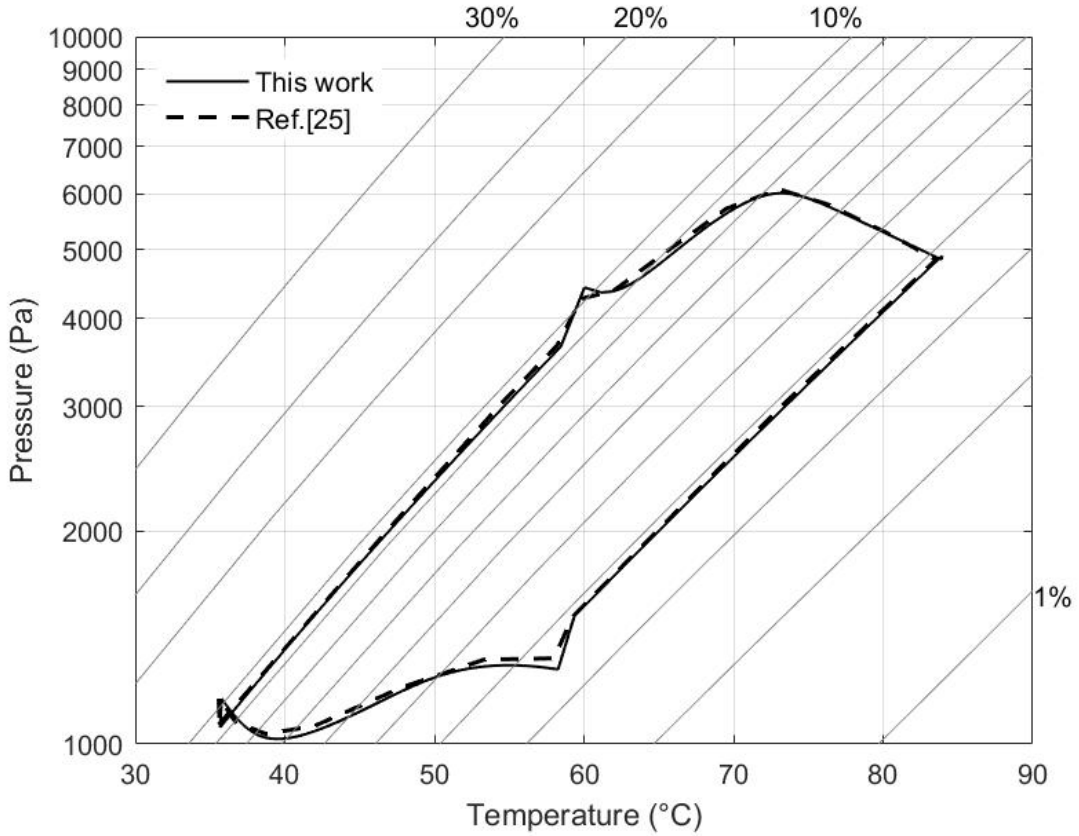

Figure 2 – Models comparison: Dühring diagrams.

The validation is completed by verifying the influence of cycle time on coefficient of performance (COP) and cooling power (CP). In fact, it is well known that excessively short cycle times negatively affect both COP and CP, due to thermal capacity and its influence on the time required to complete the temperature/pressure swing. In contrast, long cycle times promote COP but degrade CP, since the latter results from the ratio of cooling energy, whose value is limited by the bed adsorption capacity, and cycle time. As shown in Fig. 3, the COP is matched very well, whereas the models differ by a small deviation in terms of CP. However, the maximum difference is about 2%. Thus, the model validation can be considered quite satisfactory.

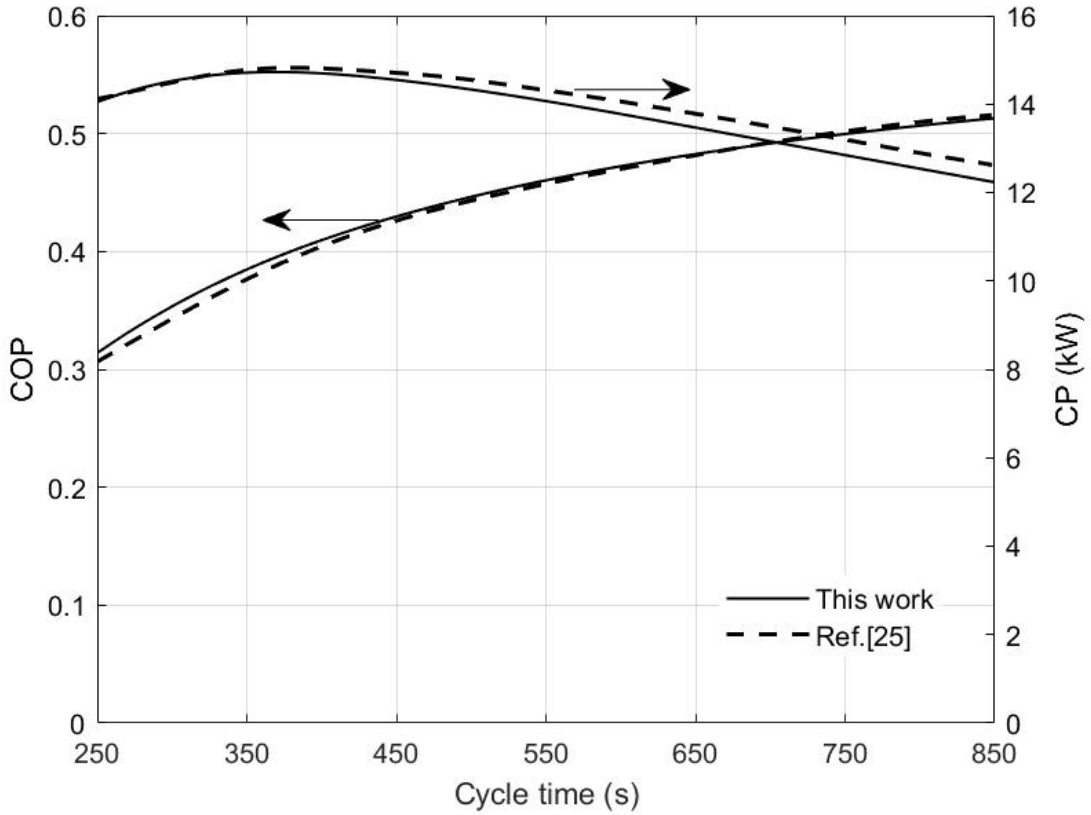

Figure 3 – Models comparison: COP and CP dependency from cycle time.

3. Cascade adsorption cycle

The operating principle of a cascade adsorption cycle constituted of a twin bed cycle and a single bed cycle is illustrated in sub-section 3.1, along with the hydraulic scheme of the system. The number of independent design parameters is reduced through scaling rules, presented in section 3.2 along with the operating conditions under which the parametric simulation study is carried out.

3.1 Operating principle

A cascade adsorption cycle is realized by combining a high temperature cycle (BED_1 and BED_2) with a low temperature cycle (BED_3). The working pair for the HT cycle is Zeolite 4A-water and that for the low temperature cycle is $CaCl_2$/Silica gel-water. The system operates in four steps, as shown in Fig. 4. During the first step, one of the high temperature beds (e.g., BED_1) performs adsorption by exchanging heat with the low temperature bed, which performs desorption, while the other high temperature bed (BED_2) is externally heated to perform desorption. In the second step, internal heat recovery between BED_1 and BED_2 takes place

and, depending on the available temperature spread, BED_1 may start to desorb and BED_2 to adsorb. Simultaneously, the low temperature bed is externally cooled in order to perform adsorption. The third and four steps replicate the first and second ones, with BED_1 and BED_2 exchanging their role. Therefore, cycle time is the sum of the durations of two consecutive steps. A qualitative representation in the Dühring diagram of the four-step cycle is presented in Fig. 5, where the dashed arrows indicate internal heat recovery. The superior performance achievable by this system is justified by the observation that, while cooling power is provided during each of the 4 steps, heat input is required only in step 1 and 3. Therefore, twice the COP of the single effect twin bed cycle is expected. However, this performance increase is obtained at the expense of a higher system complexity, a higher driving temperature, and an additional bed, which implies lower than usual specific cooling power.

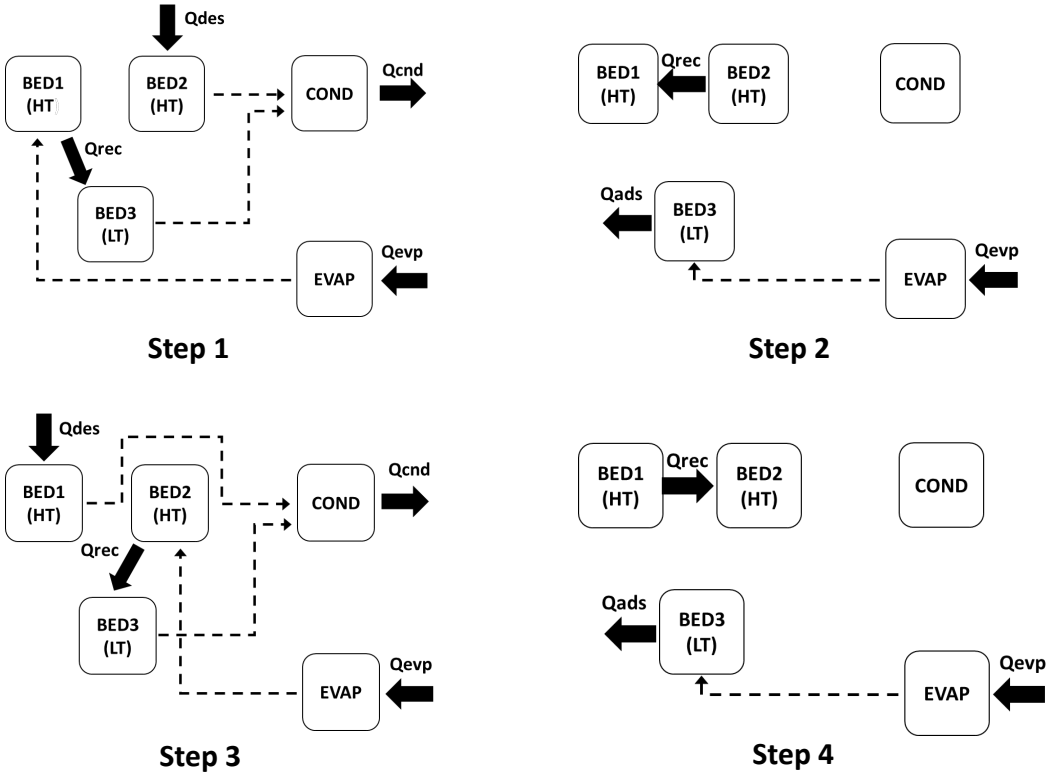

Figure 4 – Schematic of the three-bed cascade cycle operating in four steps

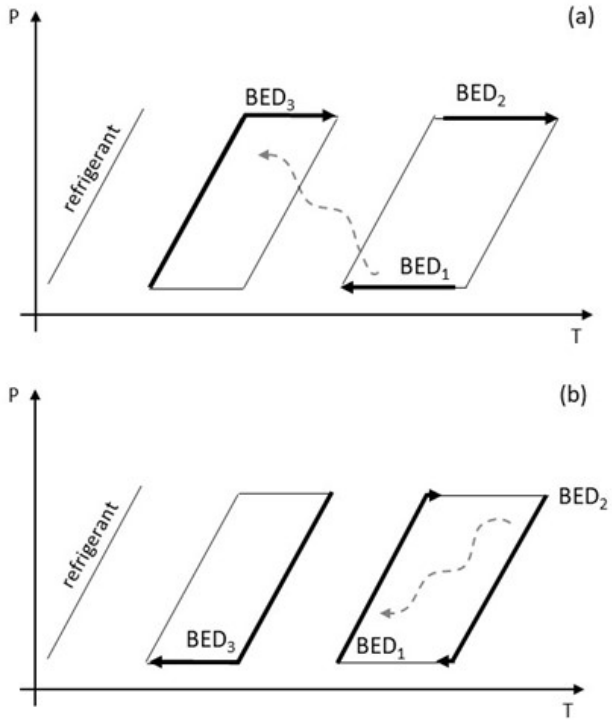

Figure 5 – Operating principle of the three-bed cascade cycle in the Dühring diagram: a) step 1, b) step 2.

The detailed hydraulic and refrigerant circuits are shown in Fig. 6. The heat input for the desorption of the high temperature beds (Q_{des}) is alternatively supplied to BED_2 (step 1) and BED_1 (step 3) through pump P_1, while the heat of adsorption of BED_1 (step 1) and BED_2 (step 3) is recovered internally to perform desorption of BED_3 through pump P_2. Changing the setting of the hydraulic valves, pump P_1,is used for internal heat recovery between BED_1 and BED_2 and pump P_2 is used to reject heat of adsorption from BED_3 (steps 2 and 4).

It should be noticed that condensation occurs simultaneously in $COND_A$ and $COND_B$, while evaporation occurs alternatively in $EVAP_A$ (step 1 and 3) and $EVAP_B$ (step 3 and 4). Therefore, a possible simplification would consist in the utilization of a common evaporator for both the LT and HT beds. Lastly, the heat transfer fluid circulating in the three beds is diathermic oil, since its property are suitable for the high temperatures required to desorb BED_1 and BED_2, while water is used as heat transfer fluid for condensers and evaporators.

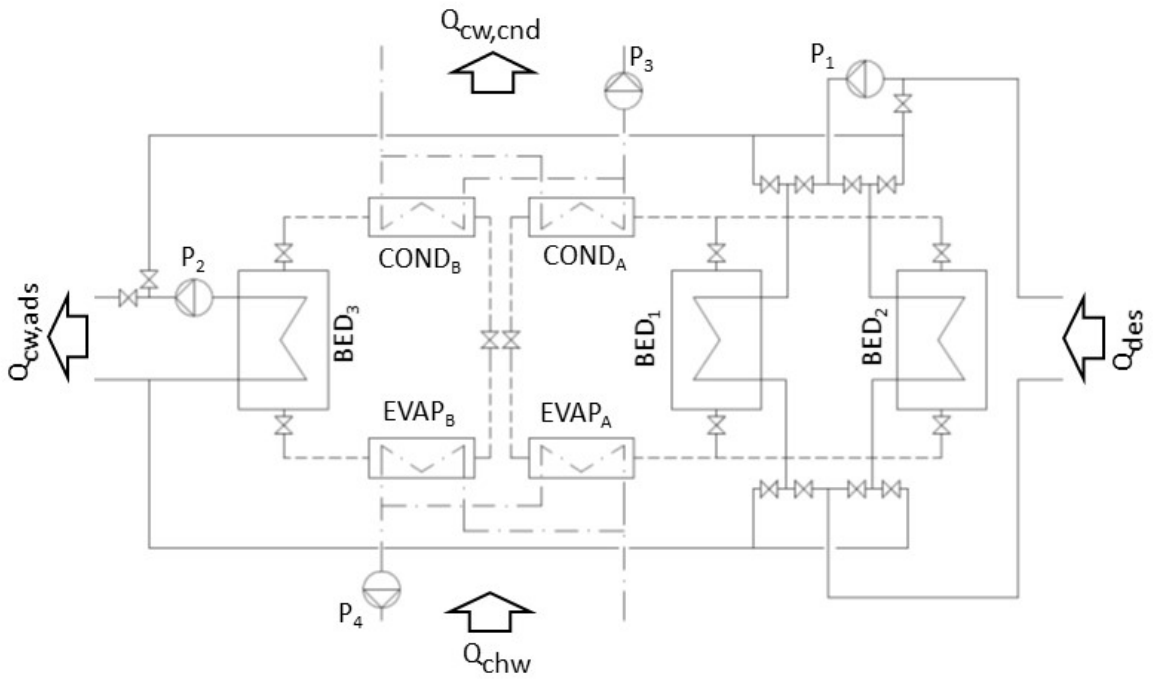

Figure 6 – Schematics of the three-bed cascade cycle.

3.2 Simulation parameters and conditions

The key parameters that are varied during the simulations are mass ratio (MR), defined as $M_{s,BED3}/M_{s,BED1}$, cycle time (t_c), equal to the sum of time of step 1 (t_1) and time of step 2 (t_2), and step time ratio (SR), equal to t_2/t_c. The parameters MR and SR are selected in addition to cycle time because, although in principle one could set MR to 1 and SR to 0.5, differences in the isotherms of the two adsorbents used in the LT and HT beds and the higher mass transfer resistance that characterizes adsorption at low temperatures make the *a priori* definition of MR and SR uncertain. All other system parameters, normalized for $M_{s,BED1} = 1$ kg, are derived based on typical values found in the literature. The mass of adsorbent is the driver for the determination of UA, Mc_{hx}, M_{htf} and $\dot{m}_{htf}$ of the three adsorption beds. Since the different masses of BED_3 and BED_1 would provide different flow rates for the heat recovery between LT bed and HT beds, the same flow rate of BED_1 is used also for BED_3 to avoid unbalanced flows during desorption and adsorption of the two HT beds. Moreover, both UA and $\dot{m}_{htf}$ are judiciously scaled to consider that literature values are achieved with water as heat transfer medium while, in the case at hand, diathermic oil is used. Concerning evaporators and condensers, their parameters are scaled according to the mass of adsorbent in the high temperature bed, since in principle their heat duties are like those of evaporator and condenser of a twin bed

single effect cycle. The complete list of normalized input parameters, calculated for a specific set of independent parameters, is shown as example in Table 2.

Table 2. Input parameters for the system components, MR=0.5.

Parameter	$BED_{1,2}$	BED_3	$COND_A$	$EVAP_A$	$COND_B$	$EVAP_B$
M_s (kg)	1	0.5	-	-	-	-
UA (W/K)	43	21.6	400	100	200	100
Mc_{hx} (J/kg)	900	630	200	100	100	100
M_{htf} (kg)	0.44	0.31	0.35	0.2	0.18	0.3
$\dot{m}_{htf}$ (kg/h)	182	182	100	80	50	80
M_r (kg)	-	-	0.26	1.06	0.13	1.06

Concerning the operating conditions of the system, the temperature of diathermic oil is set to 200 °C at the inlet of the high temperature beds (for desorption) and at 30 °C at the inlet of the low temperature bed (for adsorption). The cooling water temperature at condensers inlet is 30 °C and the chilled water temperature at evaporators inlet is 12 °C.

Lastly, the inlet and outlet valves of beds are simulated like ideal check valves. Therefore, a switching time for these valves is not required, since they automatically open and close according to the differential pressure between the beds and the connected heat exchangers.

4. Results and discussion

The optimization of the independent parameter of the cycle is presented in sub-section 4.1 and suitable system configuration are selected, with the aim of optimizing both COP and SCP. Subsequently, the cyclic steady-state behaviour of an interesting configuration is investigated in sub-section 4.2.

4.1. Cycle optimization

The influence on cycle performance of cycle time, duration of each step and the mass of adsorption material in the low temperature bed is investigated. Two performance indicators are assessed, COP and specific cooling power (SCP), which are defined as follows:

$$COP = Q_{chw}/Q_{des} \tag{17}$$

$$SCP = Q_{chw}/(M_{s,BED1} + M_{s,BED2} + M_{s,BED3}) \tag{18}$$

The results of the parametric simulation are shown in Fig. 7. It can be noticed that cycle time of 400 s is too short, causing the lowest values of COP. Comparing cycle times of 600, 800 and 1000 s, the general trend is as expected: COP increases and the SCP decreases.

At high cycle times, the differences in performance associated to different values of SR are smaller than at low cycle times. Evidently, if cycle time is long enough, the relative duration of each step becomes unessential.

Variation in MR are always important, and an optimum value of MR of about 0.6 exists at all values of cycle time and SR. In practice, in all the analysed configurations, the mass of the low temperature bed must be lower than the mass of high temperature bed to achieve relative maximum COP. The reason for the maximum COP is likely to be attributed to the difference in adsorption capacity between the LT and HT beds.

A good compromise between SCP and COP is found at cycle time of 800 s and at MR equal to 0.6. For what concerns SR, the differences among 0.40, 0.45 and 0.50 are very small. Therefore, a value of 0.5 represents a practical choice, since such value would allow parallel units to operate in tandem and provide smoother variations of the heat duties at the external heat exchangers.

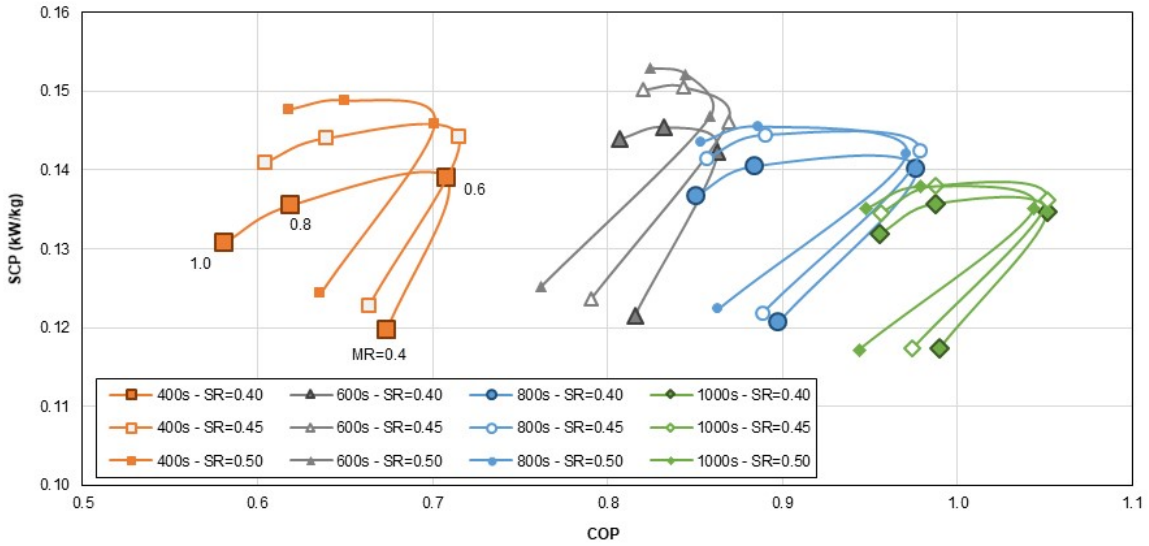

Figure 7 – Optimization of COP and SCP.

4.2. Cyclic state-state behaviour

The configuration with cycle period = 800 s, SR= 0.5 and MR=0.6 is further investigated since it shows high COP at slightly suboptimal SPC. In Fig. 8 and Fig. 9, the cyclic profiles of the three beds temperatures and those of the external heat transfer rates are shown, respectively. During step 1, BED1 exchanges heat with BED3 while BED2 is heated by the external heater. As shown by the heat transfer rates profile (see Fig. 9), cooling capacity is provided (since BED_1 performs adsorption) and considerable heat is rejected at the condensers (since both BED_2 and BED_3 perform desorption at the same time).

During step 2, heat is recovered internally between BED_1 and BED_2, while BED_3 is cooled externally. It can be noticed from Fig. 8 that the temperature difference between the two high temperature beds decreases sharply during the first seconds (from 400 to 450 s) and afterwards both temperatures settle to an asymptotic value of about 150 °C. The rapid change in the temperature derivatives point out the inception of adsorption in BED_2 and desorption in BED_1. This fact is confirmed by the profile of the heat rejected at the condensers and the considerable amount of cooling capacity provided at the evaporators (see Fig. 9). In fact, also BED_3 performs adsorption at the same time, as shown by the heat of adsorption that is rejected externally ($Q_{cw,ads}$) and thus it contributes to a large extent to cooling energy production during step 2.

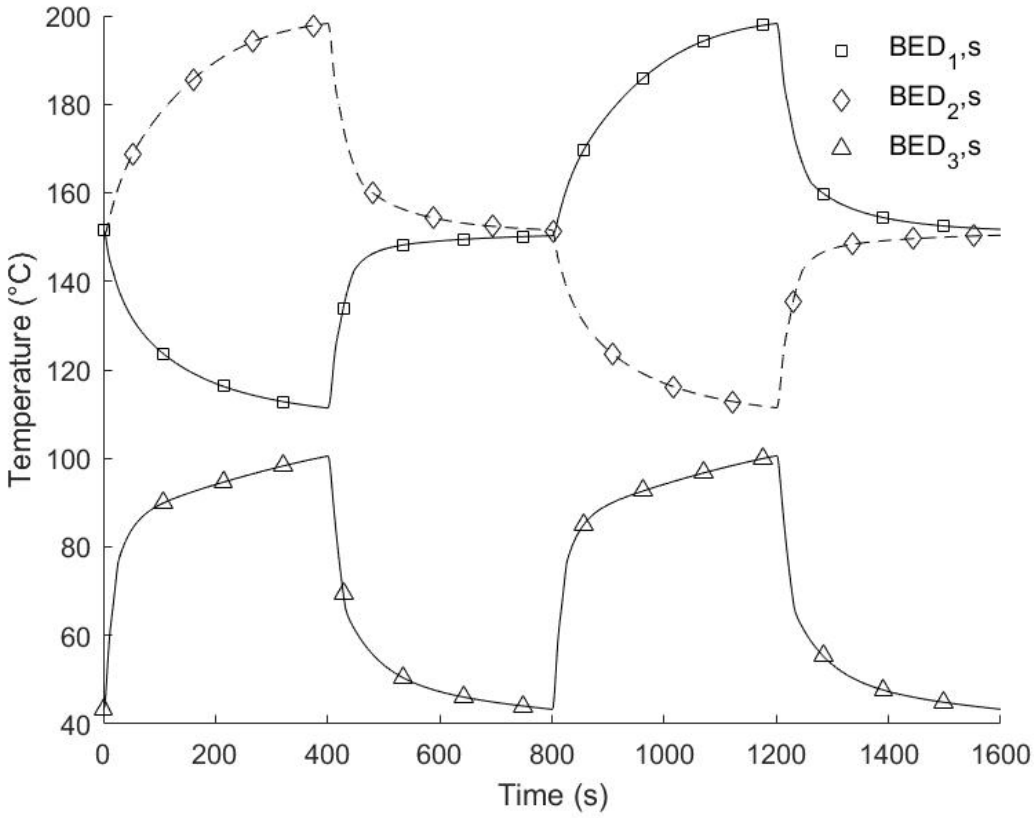

Figure 8 – Beds temperatures at cyclic steady-state.

Steps 3 and 4 are the same of steps 1 and 2, except for the roles of BED_1 and BED_2. The change in their roles can be clearly seen in Fig. 8. From this figure it can also be noticed the large temperature pinch (above 10 °C) existing for BED_3 at the end of desorption (with the high temperature beds) and adsorption (with the external heat transfer medium). This is mostly due to ineffective heat transfer, a consequence of using diathermic oil for the beds. Increasing cycle time would close the temperature gaps allowing to increase COP. However, as commented in Fig. 7, this would also cause a sharp degradation of SCP.

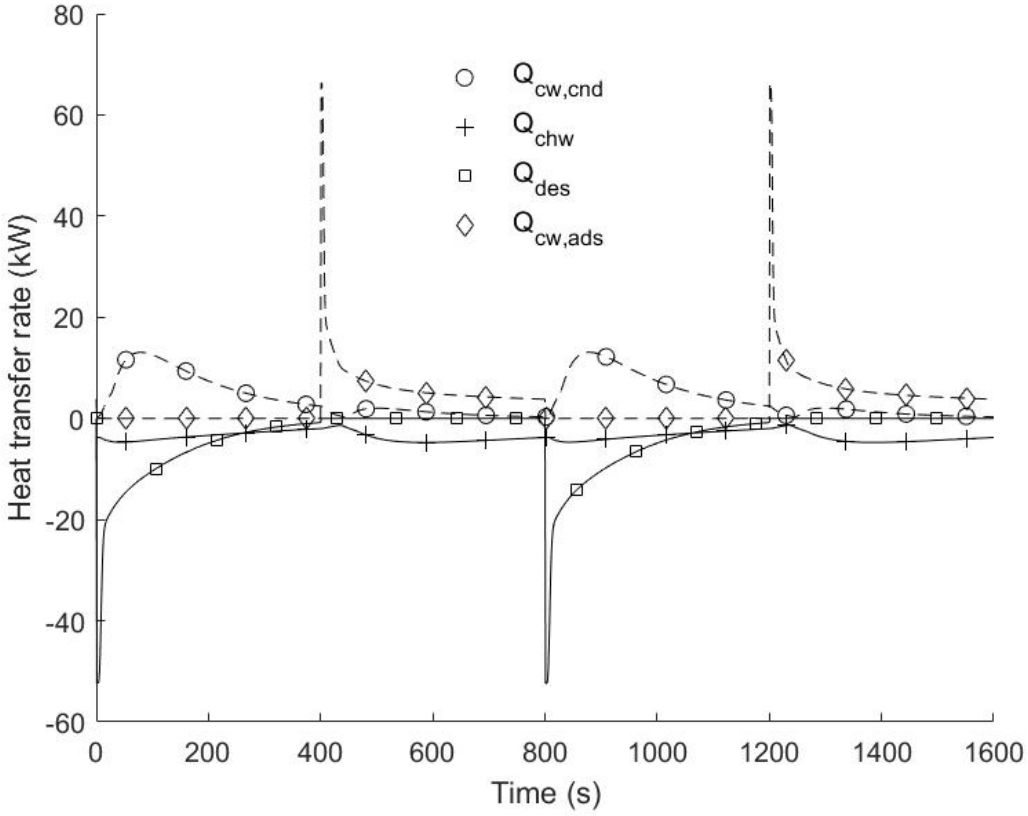

Figure 9 – External heat transfer rates at cyclic steady-state.

5. Conclusions

A capacitive sorption bed and a capacitive heat exchanger have been implemented in a modular simulation software (STACY [30]) to simulate the cyclic steady-state operation of adsorption chillers. The new features have been validated with literature data for a twin bed adsorption cycle, and model-to-model comparison of COP and CP has shown satisfactory results.

Thanks to its modular approach, the simulation software can be useful during the design and the optimization of adsorption systems. In particular, the performance of a three-bed cascade adsorption cycle that is suitable for cooling applications has been assessed in this work.

The results have shown that, for the considered cascade cycle, a potential for waste heat recovery applications at high temperature (200 °C) might exist thanks to the high values of COP (0.85 ÷ 1) and the reasonable value obtained for SCP (140 ÷ 150 W/kg). The relatively low value of SCP is not only an inherent limitation of the cycle, whose peculiar characteristic is to enhance COP at the expense of an additional adsorption bed, but also an effect of the low heat transport properties of the transfer medium

selected for the beds (diathermic oil). Therefore, higher values of SCP are likely to be achieved with an optimized design of the bed heat exchanger, by adopting thermally efficient adsorbent bed configurations (e.g. thin adsorbent coatings, adsorbent materials doped with metal- or carbon-based foams or fibers) and/or better heat transfer fluids. The detailed study of the influence of the heat transfer efficiency on the overall dynamic performance of the adsorbent system will be subject of a future work.

Moreover, the conclusions of this work are based on simplifying assumptions, namely ideal switching of the vacuum valves and absence of any thermal loss. To improve the predictive ability of the simulation tool at the stage required by model-based design and control of adsorption chillers, further modelling and validation is needed. Therefore, future work will also focus on modelling and validation of system related aspects that can have impact on the performance of real adsorption units.

Nomenclature

A	Area, m^2
c	Specific heat, J/kg·K
h	Enthalpy, J/kg
ΔH_{ads}	Isosteric heat of adsorption, J/kg
M	Mass, kg
N	Number of nodes
$\dot{m}$	Mass flow rate, kg/s
P	Pressure, Pa
Q	Heat transfer rate, W
t_c	Cycle time, s
T	Temperature, °C
U	Overall heat transfer coefficient, $W/m^2 \cdot K$
w	Sorption capacity, kg/kg
τ	Time constant, s

Abbreviations

BED Adsorption bed

$COND$ Condenser

COP Ratio of cycle averaged cooling power to heat input

CP Cycle averaged cooling power, kW

$EVAP$ Evaporator

LT Low temperature

HT High temperature

HTF Heat transfer fluid

MR Mass ratio, kg/kg

SCP Specific cooling power, kW/kg

SR Step time ratio

SW Sorbent/sorbate pair

Subscripts

bed adsorption bed

c cooling

chw chilled water

cnd condenser

cw cooling water

des desorption

eq equilibrium

evp evaporator

h heating

htf heat transfer fluid

hx heat exchanger

hw hot water

i inlet

in input

l	liquid
o	outlet
r	refrigerant
rec	recovery
s	sorbent material
sat	saturation
sw	sorbent sorbate mixture
v	vapor
w	water, sorbate

References

[1] F. Meunier, Adsorption heat powered heat pumps, Applied Thermal Engineering, 61(2) (2013) 830-836.

[2] X.H. Li, X.H. Hou, X. Zhang, Z.X. Yuan, A review on development of adsorption cooling—Novel beds and advanced cycles, Energy Conversion and Management, 94 (2015) 221-232.

[3] L. Calabrese, L.Bonaccorsi, P.Bruzzaniti, E.Proverbio, A.Freni, SAPO-34 based zeolite coatings for adsorption heat pumps, Energy, 187 (2019) 115981.

[4] Do, J., Cha, D., Park, I., Bae, J., Park, J., Hydrothermal synthesis and application of adsorbent coating for adsorption chiller, Progress in Organic Coatings, 128 (2019) 59-68.

[5] L. Bonaccorsi, L. Calabrese, A. Freni, E. Proverbio, Hydrothermal and microwave synthesis of SAPO (CHA) zeolites on aluminium foams for heat pumping applications, Microporous Mesoporous Mater., 167 (2013), pp. 30-37.

[6] A. Freni, L. Calabrese, A. Malara, P. Frontera, L. Bonaccorsi, Energy, 187 (2019) 115971.

[7] U. Wittstadt, G. Fueldner, O. Andersen, R. Herrmann, F. Schmidt, A new adsorbent composite material based on metal fiber technology and its application in adsorption heat exchangers, Energies, 8 (8) (2015) 8431-8446.

[8] B, Dawoud, Water vapor adsorption kinetics on small and full scale zeolite coated adsorbers; A comparison, Applied Thermal Engineering, 50(2), (2013) 1645-1651.

[9] U. Wittstadt, G. Füldner, E. Laurenz. A.Warlo, A. Große. R. Herrmann, L. Schnabel, W. Mittelbach, A novel adsorption module withfiber heat exchangers: Performance nalysis based on driving temperature differences, Renew. Energy, 110 (2017), 154-161.

[10] J. Ammann, B. Michel, A.R. Studart, P.W. Ruch, Sorption rate enhancement in SAPO-34 zeolite by directed mass transfer channels, International Journal of Heat and Mass Transfer
130 (2019) 25-32.

[11] A. Alahmer, S Ajib, X., Wang, Comprehensive strategies for performance improvement of adsorption air conditioning systems: A review, Renewable and Sustainable Energy Reviews, 99 (2019) 138-158.

[12] M. Pons, F. Meunier, G. Cacciola, R. E. Critoph, M. Groll, L. Puigjaner, B. Spinner, F. Ziegler, Thermodynamic based comparison of sorption systems for cooling and heat pumping, International Journal of Refrigeration, 22(1) (1999), 5-17.

[13] D.C.Wang, Z.Z.Xia, J.Y.Wu, R.Z.Wang, H.Zhai, W.D.Dou, Study of a novel silica gel–water adsorption chiller. Part I. Design and performance prediction, International Journal of Refrigeration, 28 (7) (2005) 1073-1083.

[14] Liu Y L, Wang R Z, Xia Z Z. Experimental performance of a silica gel-water adsorption chiller. Applied Thermal Engineering, 25 (23) (2005) 359–375.

[15] Y. Yu, Q. W. Pan, L. W. Wang, A small-scale silica gel-water adsorption system for domestic air conditioning and water heating by the recovery of solar energy, Frontiers in Energy, https://doi.org/10.1007/s11708-019-0623-1 (2019).

[16] Q.W. Pan, R.Z. Wang, Study on operation strategy of a silica gel-water adsorption chiller in solar cooling application Solar Energy, 172(1) (2018), 24-31.

[17] Yu I. Aristov, Adsorption dynamics in adsorptive heat transformers: review of new trends, Heat. Transf. Eng. 35 (11-12) (2014) 1014-1027.

[18] M. Pons, F. Poyelle, Adsorptive machines with advanced cycles for heat pumping or cooling applications, International Journal of Refrigeration, 22(1) (2000) 27-37.

[19] A. Akahira. K.C.A. Alam, Y. Hamamoto, A. Akisawa. T. Kashiwagi, Mass recovery adsorption refrigeration cycle—improving cooling capacity, International Journal of Refrigeration
27 (3) (2004) 225-234.

[20] B. Zajaczkowski, Optimizing performance of a three-bed adsorption chiller using new cycle time allocation and mass recovery, Applied Thermal Engineering, 100 (2016), 744-752.

[21] R.Z. Wang, Performance improvement of adsorption cooling by heat and mass recovery operation, International Journal of Refrigeration, 24 (7) (2001), 602-611.

[22] N. Ben Amar, L.M. Sun, F. Meunier. Numerical Analysis of adsorptive temperature wave regenerative heat pumps, Appl. Therm. Eng. 16, (1996) 405-418.

[23] D. Miles, S. Shelton. Design and testing of a solid sorption heat pump system, Appl. Therm. Eng. 16, (1996) 389-394.

[24] S. Szarzynski, M. Pons. A novel experimental unit for adsorptive refrigeration with heat regeneration (non uniform temperature), In: Fundamentals of Adsorption, Elsevier, 1113-1118, (1998).

[25] M.Z.I.Khan, K.C.A.Alam, B.B.Saha, A.Akisawa, T.Kashiwagi, Performance evaluation of multi-stage, multi-bed adsorption chiller employing re-heat scheme, Renewable Energy, 33 (1) (2008), 88-98.

[26] B.B. Saha, S. Koyama, T. Kashiwagi, A. Akisawa, K.C. Ng, H.T. Chua, Waste heat driven dual-mode, multi-stage, multi-bed regenerative adsorption system, Int J Refrigeration, 26 (2003), 749-757.

[27] N. Douss, F. Meunier, Experimental study of cascading adsorption cycles, Chem. Eng. Sci. R. (1989) 225–235.

[28] Y. Liu, K.C. Leong, Numerical study of a novel cascading adsorption cycle, Int. J. Refrig. 29 (2006) 250–259.

[29] A. S. Uyun, T. Miyazaki, Y. Ueda, A. Akisawa, High performance cascading adsorption refrigeration cycle with internal heat recovery driven by a low grade heat source temperature, Energies (2009), 1170–1191.

[30] M. Aprile, T. Toppi, S. Garone, M. Motta, STACY–A mathematical modelling framework for steady-state simulation of absorption cycles. Int. J. Refrig. 88 (2018), 129–140.

[31] H. T. Chua, K. C. Ng, A. Malek, T. Kashiwagi, A. Akisawa, B. B. Saha, Modeling the performance of two-bed , sillica gel-water adsorption chillers, Int. J. Refrig. 22 (1999), 194–204.

[32] H. T. Chua, K. C. Ng, A. Malek, T. Kashiwagi, A. Akisawa, B. B. Saha, Erratum to "Modeling the performance of two-bed, silica gel-water adsorption chillers" [Int. J. Refrigeration 22 (1999) 194-204], Int. J. Refrig. 31 (2008), 536.

[33] A. Freni, G. Maggio, A. Sapienza, A. Frazzica, G. Restuccia, S. Vasta, Comparative analysis of promising adsorbent/adsorbate pairs for adsorptive heat pumping, air conditioning and refrigeration, Appl. Therm. Eng. 104 (2016), 85–95.

[34] M. Pons, Ph. Grenier, A phenomenological adsorption equilibrium law extracted from experimental and theoretical considerations applied to the activated carbon+ methanol pair, Carbon 24 (5) (1986), 615–625.

[35] EC Boelman, BB Saha, T Kashiwagi, Experimental investigation of a silica gel-water adsorption refrigeration cycle – the influence of operating conditions on cooling output and COP, ASHRAE Trans Res 101(2) (1995), 358–366.